

Dust clouds and plasmoids in Saturn's Magnetosphere as seen with four *Cassini* instruments

Emil Khalisi¹

*Max-Planck-Institute for Nuclear Physics, Saupfercheckweg 1, D-69117 Heidelberg,
Germany*

Abstract

We revisit the evidence for a "dust cloud" observed by the *Cassini* spacecraft at Saturn in 2006. The data of four instruments are simultaneously compared to interpret the signatures of a coherent swarm of dust that would have remained near the equatorial plane for as long as six weeks. The conspicuous pattern, as seen in the dust counters of the Cosmic Dust Analyser (CDA), clearly repeats on three consecutive revolutions of the spacecraft. That particular cloud is estimated to about 1.36 Saturnian radii in size, and probably broadening. We also present a reconnection event from the magnetic field data (MAG) that leave behind several plasmoids like those reported from the Voyager flybys in the early 1980s. That magnetic bubbles happened at the dawn side of Saturn's magnetosphere. At their nascency, the magnetic field showed a switchover of its alignment, disruption of flux tubes and a recovery on a time scale of about 30 days. However, we cannot rule out that different events might have taken place. Empirical evidence is shown at another occasion when a plasmoid was carrying a cloud of tiny dust particles such that a connection between plasmoids and coherent dust clouds is probable.

Keywords: Dust clouds, Saturn, Cassini mission, Cosmic Dust Analyser, Magnetosphere

URL: DOI: <http://dx.doi.org/10.1016/j.asr.2016.12.030> (Emil Khalisi)

¹Corresponding author: ekhalisi@khalisi.com

1. Introduction

Interplanetary dust clouds are local density enhancements of particles of a specific mass type. They would usually be relicts of dissolved comets, debris of an asteroidal collision, ejecta from planets or moons, and a few may also go back to jet streams from active bodies, or coronal mass ejections. In the vast range of patterns, the characteristics of dust will vary on all dimensions: size, density, mass, lifetime, and more (see, e.g., [Grün *et al.* \(2004\)](#)).

During the *Pioneer* and both *Voyager* flybys at Saturn in the 1980s, regions of plasma material were found on the day-side of the Saturnian magnetosphere ([Bridge *et al.* \(1981\)](#), [Bridge *et al.* \(1982\)](#)). These are local spots of relatively dense and cold plasma at distances beyond 16 Saturnian radii ($1 R_S = 60,268$ km). In particular, *Voyager 2*'s ion spectrometer suggested that numerous of such isolated “plasma blobs” float closely to the Saturnian magnetopause. Dust grains, which would be very much more massive than plasma components, were not reported. We accidentally discovered in the *Cassini* data one striking event that showed a local enhancement of dust particles resembling a “dust blob” remaining for a few revolutions of the spacecraft ([Khalisi *et al.* \(2015\)](#)). Now, we will investigate that event in more detail throughout this paper.

Dust usually carries an electric charge, so, it seems likely that there might be regions of increased dust particles more or less tied to magnetically confined areas. An analog for such accumulations could be the Coronal Mass Ejections in the solar wind. The *Cassini* mission offers an excellent opportunity to search for similar dust clouds, more so, as the existence of the plasma blobs has already been verified. The source of plasma enhancements is still unresolved, but a plenty of mechanisms were debated. We will briefly review five of them in the next section. Thereafter, we show an example for a “dust cloud” and a “plasmoid” as well as a connection of both. For the coupling of these two types, we empirically present a multi-instrument evidence.

2. Plasma and dust models for the magnetosphere of Saturn

2.1. Sputtering

Among the first accounts on plasma concentrations at Saturn, [Frank *et al.* \(1980\)](#) came forward with ion observations made by *Pioneer 11* in 1979. They identified a torus of cold hydrogen (H^+) and oxygen ions (O^{2+} and O^{3+}) in the distance range of ≈ 4 – $16 R_S$. They proposed a sputtering

mechanism from two sources: the Saturnian rings as the primary source as well as the ice moons Dione and Tethys as secondary sources. Almost three decades later, the Cassini Plasma Spectrometer (CAPS) confirmed the existence of the plasma injections from these moons (Burch *et al.* (2007)). The injections are very localized, while the inherent electrons have pitch-angle distributions characteristic for a trapped population.

Meanwhile, the geologically active moon Enceladus became known as a significant contributor of dust, water ice, salty contaminations, and charged particles, all of which would further disintegrate in the tenuous environment (Porco *et al.* (2006)). Enceladus attracted more notice and is considered as the main source of ejecta now.

2.2. Titan wake

The second explanation on those density enhancements was associated with a plasma wake from Titan. Although lacking a magnetic field of its own, Titan’s atmosphere is known as an ion source (Bridge *et al.* (1981)). From *Voyager*’s plasma measurements, Hartle *et al.* (1982) exemplified that the wake will be produced as a result of the interaction of Saturn’s magnetosphere with Titan’s induced ionosphere, in a similar way as the interaction of Venus with the solar wind. The wake would be draped in the moon’s quasi-magnetospheric tail, and it coincides with an abrupt lack of high energy electrons (>700 eV), called the electron “bite-out” region. As evolving on its backside sector, the wake arises preferably on the sunward side when Titan is exposed stronger to the variable shock front of Saturn’s magnetosphere (Fig. 6 of Hartle *et al.* (1982)). In some rare cases, Titan would entirely leave Saturn’s asymmetric magnetic field and be shocked directly by the solar wind. Then, the solar wind pressure is likely to evoke reconnection processes. Unlike Venus or Mars, all these interactions turn out very complex in the special case of Titan, for its atmosphere is affected by both Sun and Saturn (see Bertucci *et al.* (2011)).

A plasma wake can acquire a meandering shape due to its stochastic radial motion (expansion, contraction of the entire magnetosphere of Saturn) in response to the changing solar wind pressure. If it remains identifiable for a time longer than a planetary rotation, it may wrap up itself and stay in the vicinity of Titan. Thus, the *Voyager* spacecraft could have intercepted the same plasma wake more than once and mocked several density enhancements (Bridge *et al.* (1981)). Two decades later, the *Cassini* spacecraft confirmed different plasma populations during two close Titan flybys in 2004 (Szego *et al.* (2005)). The populations were found drifting as far as $1 R_S$ (or 20 Titan radii) from the moon itself. However, it was not discernible whether the same

furled structure was traversed, or different particle flows were generated at different times, or even both.

2.3. Detachments from the magnetospheric sheet

A third model was presented by [Goertz \(1983\)](#). He pointed out that the observed plasma “islands” could be detached from the magnetospheric sheet of Saturn. This idea is motivated by [Hill \(1976\)](#) on flux-tubes in a centrifugally distorted magnetic field. A flux-tube becomes unstable when its plasma content is a decreasing function of the distance from the spin axis. The theory was successfully applied to the outer magnetosphere of Jupiter. For Saturn, such extensions would happen on the boundary of the magnetospheric sheet to the outer magnetosphere, i.e. at about 16 or 17 R_S . [Goertz \(1983\)](#) compared the enclosed bubbles of tailward-moving plasma, which he called “plasmoids”, with the separating magnetic blobs already known from the Earth’s magnetosphere.

In the same year, [Sittler *et al.* \(1983\)](#) presented a comprehensive analysis of the plasma observations and sketched a magnetospheric environment around Saturn with three fundamentally different regions: the inner plasma torus ($< 7 R_S$), the extended plasma sheet ($7\text{--}15 R_S$), and a hot outer magnetosphere ($> 15 R_S$) which extends right down to the magnetopause. The *Voyager* data implied that the disturbances display an anti-correlated nature of electron properties (density and temperature): Hot and more tenuous electrons drift from the outer magnetosphere inwards, while a cool and rather dense electron component from the inner torus migrates outwards, combined with heating. So, there exists an inward and outward transport of plasma electrons.

The morphology of the magnetospheric profile was essentially confirmed by *Cassini* ([Arridge *et al.* \(2007\)](#)). The magnetometer observations also revealed those plasmoids. The examples presented originate from a radial distance of $\approx 22 R_S$. The structures were interpreted as multiple crossings of a rippled or displaced current sheet caused by solar wind variations. Three more plasmoids were identified in the magnetic tail at distances as far as $40 R_S$ ([Hill *et al.* \(2008\)](#)).

The model of plasma detachments does not necessarily contradict the Titan-associated wake model above (Sect. 2.2), for both are consistent with gradual aging effects. [Sittler *et al.* \(1983\)](#) estimated the time scale for the dispersal to be a few Kronian rotation periods. As [Goertz \(1983\)](#) pointed out, a Titan plume would remain stable as long as it moved very slowly. When speeding up, the velocity shear across the wake can generate a Kelvin-Helmholtz instability which will lead to a mixing of the slow wake and

fast background plasma. Also, the centrifugal instability will cause a rapid dispersal in radial direction. It is even likely that the combined effects account for the diffusion.

The sources of these plasma injections remain unknown, but they seem to be randomly distributed in both local time and Saturnian longitude. Another argument in favor are the matching values of the peak densities of both plasma blobs and in the plasma sheet.

Last but not least, [Sittler *et al.* \(1983\)](#) showed that the attenuation of electron energies was correlated with micron-sized dust particles. In particular, the authors referred to the inner plasma torus inside of $5 R_S$, though such signatures would easily apply to any diamagnetic shielding of neutral material in general. The range of the attenuation will be approximately equal to the diameter of the dust particles.

2.4. Hyperion as dust source

A new angle of view was thrown in by [Banaszkiewicz & Krivov \(1997\)](#). Using numerical simulations, the authors argued that Hyperion, at $24 R_S$, would possibly serve as a dust supplier for Titan. Initially, the dust particles of a few micro-meter in size, originating from Hyperion, are locked in a 4:3 mean motion resonance with Titan and forming a stable dust belt. That resonance will be destroyed by the solar radiation pressure, and, to a much smaller share (less than 1%), by the plasma drag force ([Krivov & Banaszkiewicz \(2001\)](#)). Once the resonance is broken, the orbits of the dust particles become unstable and stratify themselves by mass: the larger ones of $\approx 5\mu\text{m}$ segregate inwards and collide with Titan, the smaller ones will escape out of the system.

Since both Hyperion and Titan move close to the boundary of the dayward magnetosphere of Saturn, the region between the two moons is filled with low density, hot, and subsonic plasma. In this region, the interaction occurs between the dust particles and the plasma: The much faster moving plasma of ions exposes a drag force on the dust grains ([Banaszkiewicz & Krivov \(1997\)](#)). However, at the time of designing the theory, *Cassini* was still en route to Saturn and the parameters of the dust as well as the assumed yields of ejecta from Hyperion were poorly known. Many assessments were uncertain.

Later, [Kennedy *et al.* \(2011\)](#) looked for such dust swarms in the far-off field at Saturn (>100 Saturnian radii, R_S) deploying observations of the *Spitzer Space Telescope* in the infrared. A large-scale cloud, that could be attributed to an irregular satellite or other cosmic origin, was not found definitely.

2.5. Two-cell plasma convection

A fifth approach to explain the density enhancements in the outer magnetosphere was presented by [Gurnett *et al.* \(2007\)](#) when studying the Saturn kilometric radiation (SKR). The SKR is an intense radio emission from the auroral zones, analogous to the auroral radiation on Earth. Their model goes without artificial relations to moons or their ambiances. The heart of [Gurnett *et al.* \(2007\)](#)'s concept was a two-cell convection emerging between the neutral gas torus at the orbit of Enceladus and the magnetospheric plasma sheet.

The mass loss from the geysers of Enceladus (distance: $3.95 R_S$) feeds the neutral gas torus all the way along its orbit. As the plasma passes outward through the inner edge of the neutral gas torus, it picks up newly ionized particles from the torus and thereby increases its density. The density remains lower on the opposite longitude, thus, the centrifugal forces become different. This difference drives a large convection cell on either flanks of the planet (see Fig. 3 of [Gurnett *et al.*, 2007](#)). The rapid rotation of the plasma disk and the constrained motion of the particles to the magnetic field lines act additionally to concentrate the plasma near the equatorial plane.

As both convection cells rotate, their outflow produces perturbations that drift into the outer magnetosphere. The associated perturbations in the magnetic field develop a phase lag. By the time these perturbations reach the magnetopause at $\approx 20 R_S$, they appear at the morning side of the planet, where the SKR would be generated. This would be consistent with the fact that the electron density is often different on the inbound and outbound arcs of the *Cassini* trajectory, in particular in the vicinity of Enceladus ([Gurnett *et al.* \(2007\)](#)). Thus, the period of the SKR modulation proved to be locked to the variation of the plasma density in that inner region of the magnetosphere.

In fact, *Ulysses* was able to sense the SKR from Saturn. The observations by [Galopeau & Lecacheux \(2000\)](#) showed that the SKR period lengthened by 1% on an annual time scale during the years from 1994 to 1997. For this long-term variations, [Gurnett *et al.* \(2007\)](#) suggested the seasonal effect of the altering solar inclination angle which affects the conductivity of the plasma disk: The illumination of the Southern hemisphere increases the conductivity of its ionosphere, which, in turn, governs a number of other phenomena including the poleward motion of flux, the corresponding aurora with its SKR, and even connects farther out to the plasma disk.

Almost the same conclusion was given by [Goldreich & Farmer \(2007\)](#) who found that the SKR must be supported by currents external to the planetary

body. They also rested the source of the varying SKR upon the coupling of the outflowing plasma and magnetic field close to the orbit of Enceladus. A current would produce a non-axisymmetric component to the intrinsic magnetic field of the planet, which itself should be symmetric because of its perfect axis alignment with the rotational axis. To sum up this model: The external magnetic field suffers a break in symmetry due to the centrifugally driven convection.

3. Data basis and orbits

The *Cassini* orbiter is in the favorable situation to exploit the dynamics in the magnetosphere in detail. The multi-instrumental view opens up a new picture to the precise topographical survey of the magnetospheric regions. We adopt the model of radial distances by [Sittler *et al.* \(1983\)](#) which was improved by [André *et al.* \(2008\)](#).

The key parameters of our study are provided by the MAPSview database. We employed the following instrumental data:

- CDA: impact rate r'_{all} of the registered dust events per 64 s, see [Khalisi *et al.* \(2015\)](#) for details.
- CAPS: electron density n_e , electron velocity v_e , and pressure P_e (EMNT parameter); and the same for ions, n_i , v_i , P_i (IMNT parameter), if present.
- MAG: strength of the magnetic field $|\mathbf{B}|$ plus its three components x , y , and z in the kronocentric solar-magnetospheric (KSM) coordinate system.
- RPWS: qualitative radio signals in the frequency bands of 1 Hz, 10 Hz, 100 Hz, 1 kHz, and 10 kHz.
- TRAJ: additionally, the current position of *Cassini* from Saturn.

Most parameters have a resolution of ≈ 1 min of time, except some very few cases when the instrument was out of its nominal operation. The CDA and CAPS are directional instruments, and their data has to be corrected for the current pointing. RPWS and MAG are not reliant on the spacecraft attitude and have the advantage of a continuous measurement of their respective signals throughout the orbit. In particular, the components of the \mathbf{B} -vector give important clues to the alignment of the magnetic field.

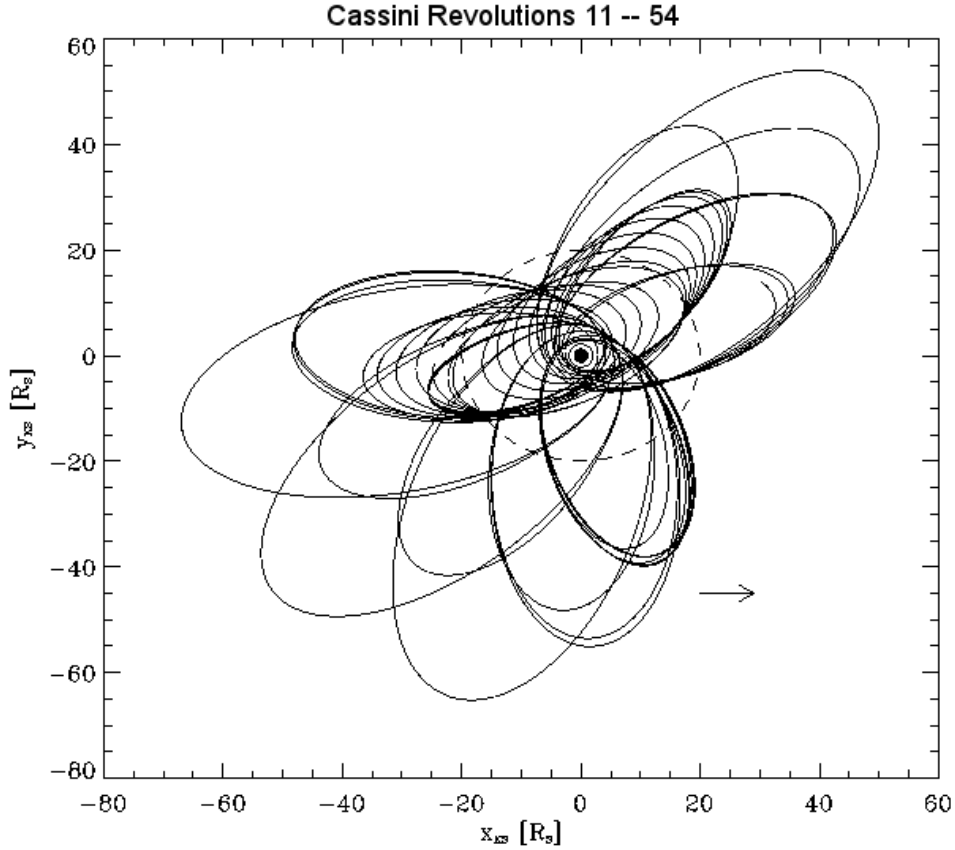


Figure 1: Projection of *Cassini*'s Revolutions #011–054 (September 2005 to December 2007) on the ring plane (top view). The arrow points in the direction of the Sun. The dashed circle marks the orbit of Titan.

Our analysis spans the *Cassini* Revolutions #11–54 (DOYs 186/2005 till 361/2007), a total of 905 days. The state of the Saturnian magnetosphere was evaluated by [Achilleos *et al.* \(2008\)](#) for the first Revolutions #7–14, which had an inclination of $i = 21^\circ$. We supplement their analysis by 40 more revolutions and put our focus to the equatorial plane ($i < \pm 5^\circ$). Figure 1 shows the projection of the orbits onto the ring plane in a Saturn-centred coordinate system. The Sun was to right hand side (arrow), illuminating the Southern hemisphere; it was below the plane at an angle of $\approx 20\text{--}10^\circ$ getting increasingly shallower.

The orbital inclinations of *Cassini*'s trajectory changed during its tour. The equatorial plane was traversed at the dusk side for the Revolutions

#15–26, while the line of apsides turned slowly to the magnetotail. At the interim Revolutions #27–46 the orbits suffered from high inclinations ($i > 25^\circ$), which we redlined from this particular analysis. When the orbits were re-tilted to the ring plane for the Revolutions #47–52, *Cassini* already transited the evening side of the magnetosphere. A disturbance from Jupiter’s magnetic field was not given, for it had outpaced Saturn back in 2000 and, now, was a quarter of its orbit ahead. Also, the solar activity passed its maximum in 2000, and was subsiding. Therefore, such “external effects” can be neglected with regard to the years 2005 to 2007, and even so at the distance of Saturn.

4. Topography of the magnetosphere

Our approach was such that we firstly determined the state of the magnetosphere at each revolution. The electron density in the solar wind reveals stable at values of $n_e \approx 10^{-1} \text{ cm}^{-3}$, as are the electron velocities v_e at $\approx 20\text{--}40 \text{ km/s}$. Though the electrons are thermal velocities, they provide continuous data and a resolution on 1-min-scale, while the ion data are often missing in the data base. The electron data proved beneficial to distinguish the borders of the magnetospheric regions. The interplanetary magnetic field strength is usually $|\mathbf{B}| \approx 0.5\text{--}1.0 \text{ nT}$ at the distance of Saturn.

The magnetopause of Saturn is identified best by a sharp drop of n_e and a steep rise of v_e . Simultaneously, $|\mathbf{B}|$ jumps to 4–5 nT and the B_z -component turns negative. The B-values at the entry of the magnetopause do vary strongly upon local conditions. In a number of cases, when the spacecraft sojourned near the magnetopause, we observed a swaying magnetic boundary (multiple crossings of the magnetopause); or an accumulation of dust particles at the bow shock; or various detached plasmoidal regions; or a sudden depletion of electrons. The whole magnetopause appears very vivid, complex, and looks different at almost each passage. On the other hand, some dynamical phenomena show a surprisingly stable pattern that remain as long as several revolutions of *Cassini*. Therefore, the identification of some features inside the magnetosphere turns out ambiguous. [André *et al.* \(2008\)](#) confined four regions which we re-examined in our broader sample:

- the innermost plasma disk,
- outer plasma disk,
- plasma sheet (at radii $\approx 7\text{--}16 R_S$),
- and the hot outer magnetosphere reaching out to the magnetopause.

Table 1: Magnetospheric features and their characteristics for distinguishing the regions amid the instrumental data.

	MAG	CAPS
solar wind	$ \mathbf{B} \approx 0.5 - 1.5 \text{ nT}$	$n_e \approx 10^{-1} \text{ cm}^{-3}$, stable $v_e \approx 20 - 40 \text{ km/s}$
magnetopause	$ \mathbf{B} $ abrupt rise to $\approx 4-5 \text{ nT}$ B_z sharp kink to negative	n_e abrupt drop by $10-100\times$ v_e upward jump by $10\times$
magnetic cushion	co-rotating B_y	$n_e \ll 10^{-1} \text{ cm}^{-3}$, fluctuating $v_e \gg 10^2 \text{ km/s}$, unstable
plasma sheet	all B -components $\approx \text{const.}$ low variance of $ \mathbf{B} $, stable	n_e small rise, less fluctuating v_e small drop
outer plasma disk	(B_y first minimum)	n_e exceeding 1 cm^{-3} $P_e \approx 0.5 \text{ eV/cm}^{-3}$
inner plasma disk	(B_y second minimum)	$n_i > 100 \text{ cm}^{-3}$ P_i rising by factor $5-10$

The latter region has been tagged as ‘‘magnetic cushion’’ recently (Delamere *et al.* (2015)), as the processes between the current sheet and the magnetopause are not well understood in case of Saturn. The cushion behaves like a reservoir of magnetic flux balancing the centrifugal and mechanical stress when the magnetodisc re-structures itself dynamically under the variable solar wind conditions.

When the spacecraft entered any of these magnetospheric regions, the magnetometer (MAG) and plasma instrument (CAPS) displayed some characteristics that are summarized in Table 1. The features represent a very rough indication and are based upon the comparison of many orbits.

Figure 2 displays the points of entering and leaving the respective region during the Revolutions #15–26 and #47–53, as *Cassini* flew its first two bunches of equatorial orbits (inclination $i < 5^\circ$). In an edge-on view, Figure 3 shows these features for all Revolutions (#11–54). The Sun reduced its angle of illumination from -20° (arrow) to -10° during the time span considered in this study (mid-2005 to 2007).

5. Examples of dust clouds

We searched the whole data sample for patterns that repeatedly appeared in three or more subsequent revolutions. Particularly, we put our focus on

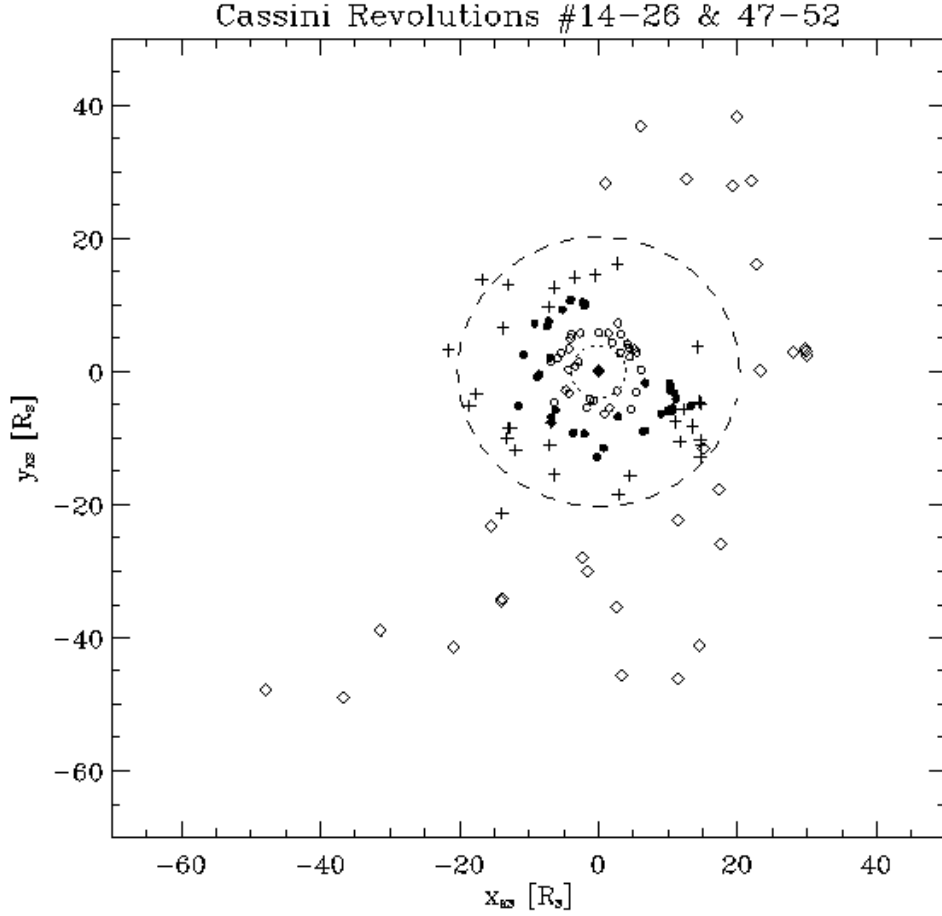


Figure 2: Crossings of the magnetospheric features with the trajectory lines of Figure 1 omitted. Shown are the boundaries of the magnetopause (diamonds), plasma sheet (black circles), outer disk (crosses), and the inner disk (small points), with all revolutions performed close to the equatorial plane.

dust particles of the CDA. An intriguing pattern was presented by [Khalisi *et al.* \(2015\)](#) for the Revolutions 26–29. Here, we revisit that data and supplement the evidence in the scope of additional instruments.

5.1. Three-peaked dust pattern at Rev. 26–29

Cassini approached its perikronium in Revolution #26 down from the magnetotail, while the magnetic field was rather quiet ($|\mathbf{B}| \approx 5$ nT), but slowly rising when approaching the inner regions. In the far-off space beyond $20 R_S$, [Arridge *et al.* \(2009\)](#) identified several crossing events of the

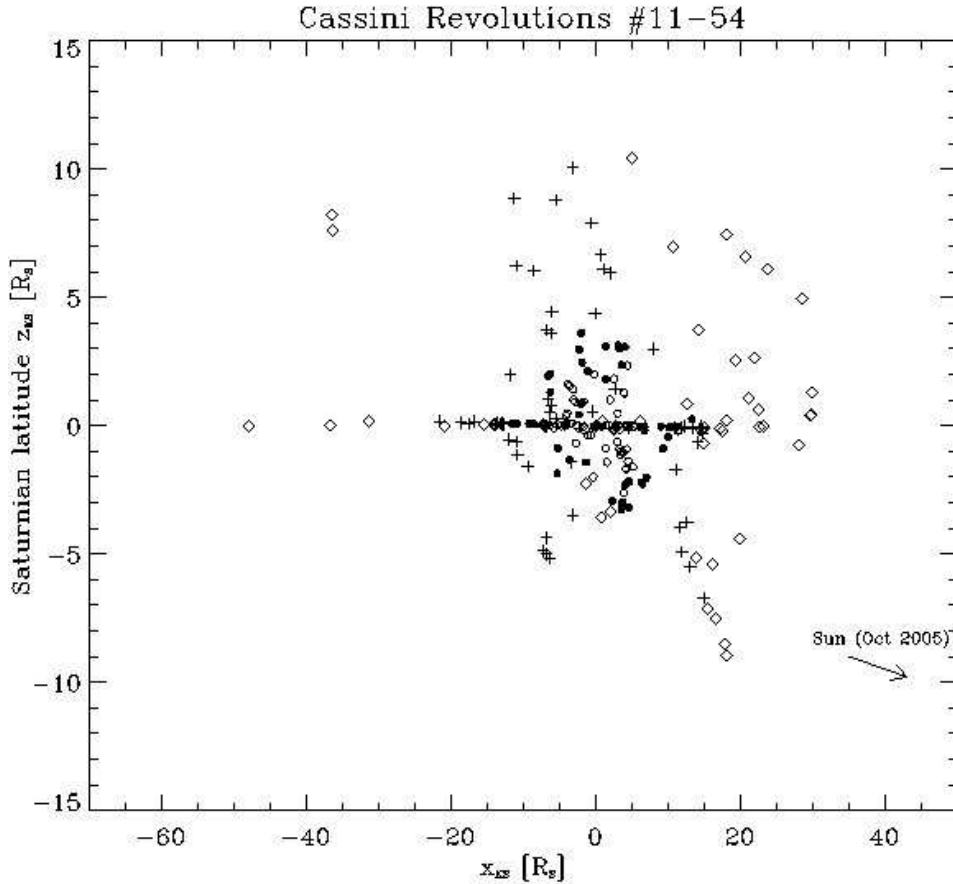


Figure 3: Vertical profile of the magnetopause (diamonds), the plasma sheet (black circles), the outer disk (crosses), and the inner disk (dots) for all Revolutions #11–54 (July 2005 – Dec 2007).

current sheet. On DOY 203.02 of 2006 a very close flyby of Titan (T16, distance: 950 km) took place. This passage was accompanied by a vigorous disturbance in all instruments (Figure 5). The magnetic data clearly shows how *Cassini* crossed the moon’s induced ionosphere. Right after the passage, the spacecraft changed its sequence of equatorial orbits and set in for a number of inclined orbits. On four consecutive revolutions, #26–29, it traversed almost the same spot in the Saturnian space (Fig. 4). On the first of these (#26), the ring plane of Saturn was crossed about two hours after that Titan flyby (DOY=203.11).

Then the CDA data revealed three conspicuous peaks of impacting particles

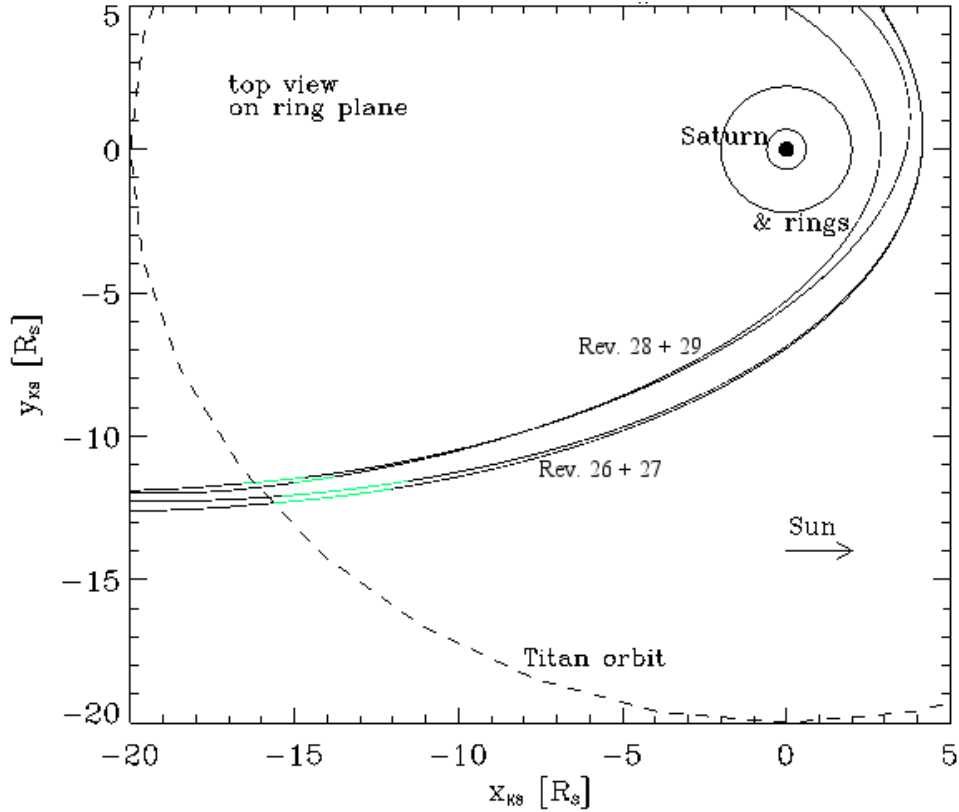


Figure 4: Trajectories of the *Cassini* Revolutions #26–29 (July–Sept 2006). The region of the dustcloud is highlighted green.

at DOY 203.17, 203.41, and a broad one around 203.70 (Fig. 5). The latter one happened during the communication period with Earth, when the probe carried out “rolls” while scanning the sky for dust impacts. From the second and third panel of Figure 5 it is seen that twice as much impacts were registered on the instrument housing (so-called “Wall events”) than on the main sensitive area (“CAT + IIT events”). That means that most particles entered the device from a direction deviating from the Kepler-RAM. The ratio of both rates would reflect the angle α between the two flows:

$$\frac{r_{\text{CAT}} + r_{\text{IIT}}}{r_{\text{Wall}}} = \cos \alpha. \quad (1)$$

A rough estimate yields that the particle cloud drifts toward $\alpha \approx 25^\circ$ relative to the Kepler-RAM. Here, we accumulated the few available data

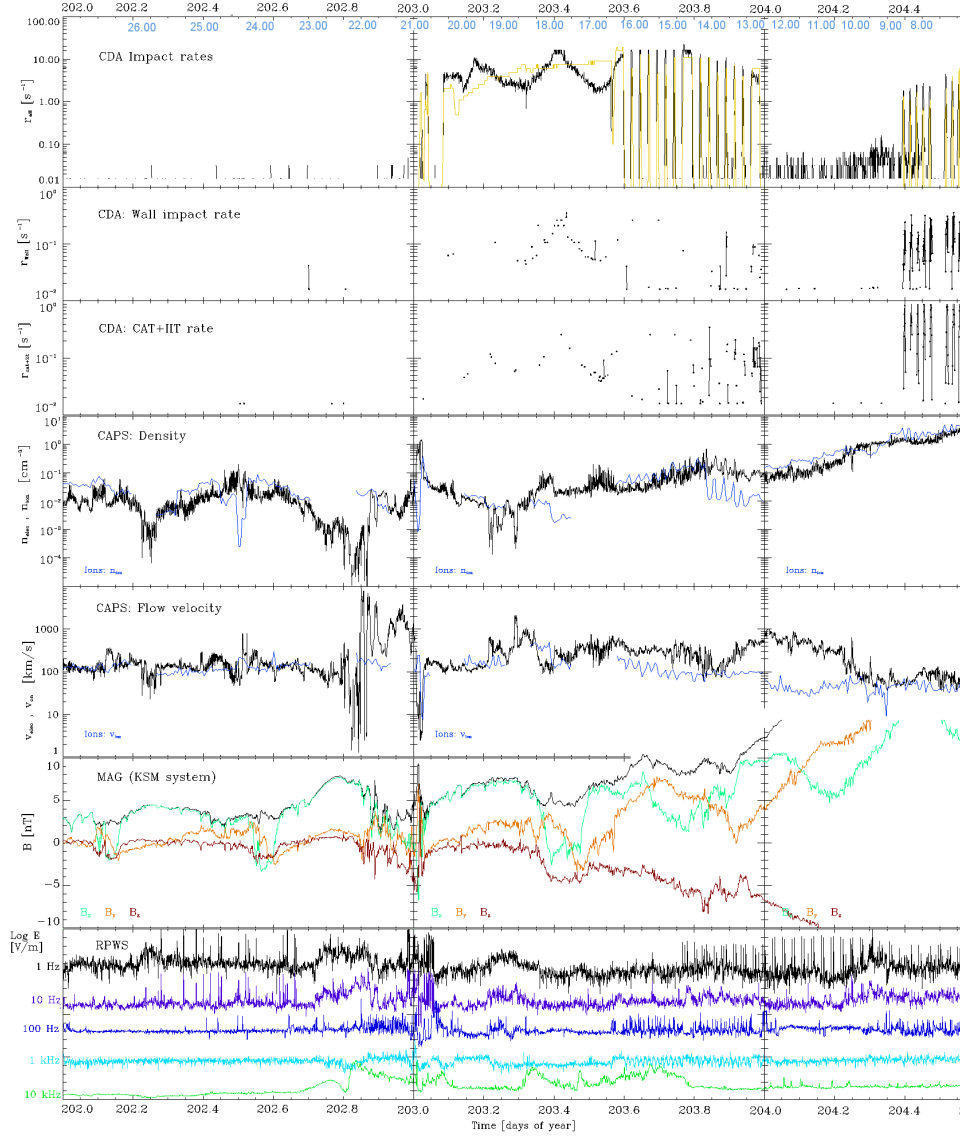


Figure 5: Comparison of four *Cassini* instruments for Revolution #26 in July 2006. *Uppermost panel*: Total impact rate r_{all} of all impacts on the CDA (black line) as well as the sensitive area (yellow line) exhibited to the Kepler-RAM. Distances from Saturn in R_s are ticked in blue colour. *Second + third panel*: Impact rates at the instrument housing (Wall) and the main targets (CAT + IIT), respectively. *Forth and fifth panel*: Densities of electrons (black) as well as ions (blue) and their velocities from the CAPS instrument. *Sixth panel*: Magnetic field strength $|\mathbf{B}|$ (black) with their spacial components. *Bottom panel*: Five signals of the lower frequency bands from the radio and plasma data (RPWS) in arbitrary units.

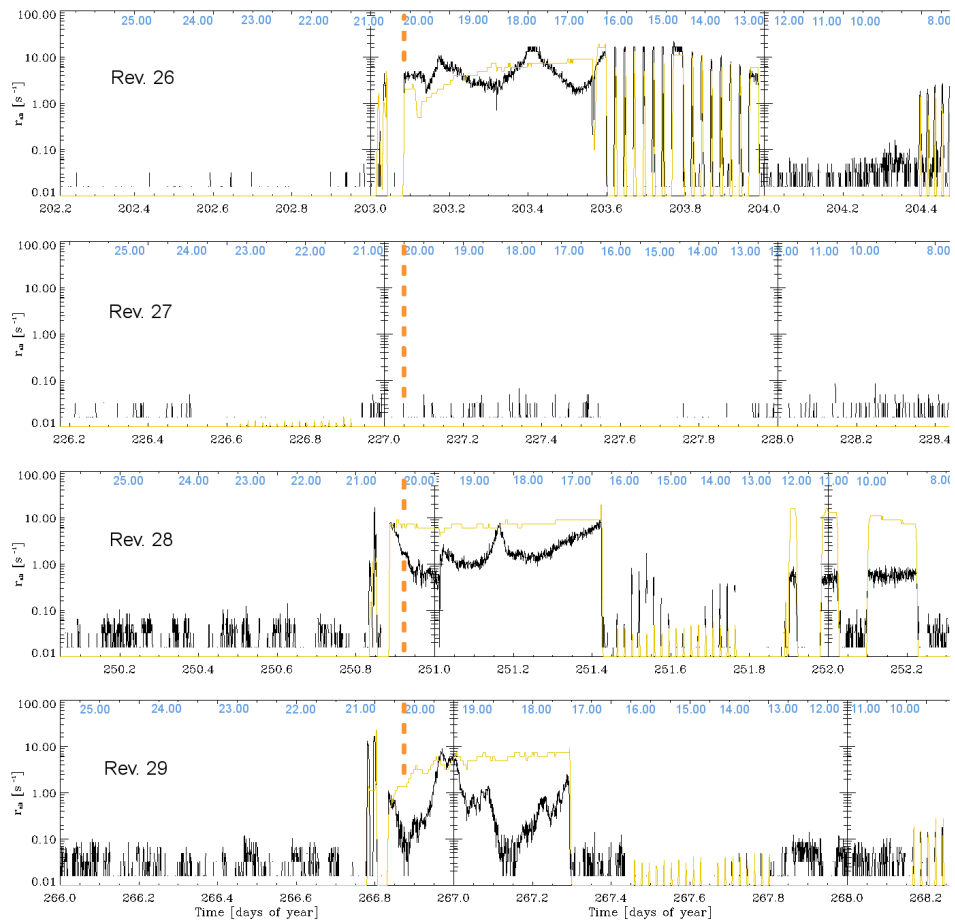


Figure 6: Dust rates and the exposed area (yellow) of the CDA for the Revolutions 026–029 (July – Sept 2006). The panels were aligned to the Titan orbit (orange dotted line). The current distance from Saturn is given at the upper axis with blue marks.

Table 2: Time markers T and distances d [in R_S] for the two main dust peaks during the orbits 26 and 28, respectively. See also Figure 4.

	Minimum	Maximum	Minimum	Maximum	Minimum
$T_{26=}$	203.14	203.175	203.31	203.41	203.525
$d_{26=}$	19.90	19.64	18.60	17.80	16.86
$T_{28=}$	251.01	251.02	251.08	251.16	251.24
$d_{28=}$	19.65	19.58	19.15	18.56	17.96

points between $T = 203.30$ and 203.55 to intervals of 30 min and computed the averages. The second dust peak coincides with a perturbation of the magnetic field, as can be seen in the sixth panel of Figure 5. It is also conceivable that a magnetic compression region, filled with dust particles, could have passed the spacecraft.

A comparison of the dust rates for the subsequent *Cassini* revolutions is shown in the next Figures. The second panel of Fig. 6 reveals that the CDA pointed to an unsuitable direction, away from the Kepler-RAM. A few “accidental” impacts still made it for measurement in the time period under consideration, i.e. from $T \approx 227.10$ to 227.55 . An enhancement of dust particles can be sensed.

At the third return to that same spot of space (third panel of Fig. 6), the signals resembled those of Revolution #26 again. The three-peaked pattern can be identified at $DOY = 251.02$, 251.16 , and 251.65 . Finally, at Revolution #29, the orbit inclination of the spacecraft had already been increased by some 10° , thus, *Cassini* must have transited the Southern parts of that dust cloud.

Examining the two front peaks separately, one finds that both have experienced an apparent compression and moved outwards (Tab. 2). The prior peak was squeezed by factor of 3, and the later by 1.5.

The second peak seems to approach faster, pushing the prior. The front side of the first pile appears steep in Revolution 26, while its tail runs out shallower. But then, in Revolution 28, the second pile compresses the fore-running and could possibly have merged into it by the time of Revolution #29. Since the spacecraft changed its orbit inclination, it would have traversed a different part of that cloud then. From the time stamps of entering and leaving the cloud, the extent of both patterns can be estimated to $\approx 82,500$ km or $1.36 R_S$.

5.2. Pulsating magnetosphere at Rev. 15–18

A magnetic reconnection event in the magnetosphere was observed during the Revolutions #15–18 in late 2005. We claim that the process persisted for several days and left behind disrupted plasmoids. The data of three consecutive revolutions resemble a “respiring magnetopause”. The relicts of that process stayed as long as 35 days – much longer than the reconnection events we would expect from Earth’s magnetosphere.

The three panels of Figure 7 show the magnetic field data of the Revolutions #15–17, and they are adjusted to the distance scale, which is given at the uppermost axis in blue ticks. *Cassini* was in the equatorial plane with the line of its apoapsis pointing to the dawn side. It passed almost the same spot of the Saturnian coordinate space for the next five revolutions. The spacecraft had already struck the magnetosphere at distance $d = 37.77 R_S$ on DOY = 260.98 (not shown here). The B_z -component had switched from positive to negative values of $\approx \pm 5$ nT at various times (shaded gray and marked with letters a, b, and c), before remaining negative at distance $d = 22.65 R_S$ on DOY = 264.72. This marked the final entering into the magnetosphere.

At the next return (#16, middle panel), most of the positive B_z -regions turned to segments of high magnetic turbulence. They are still visible in the intervals between the gray areas; the most conspicuous one appeared still reconnecting during DOY 281. The gray areas became detached plasmoids in a compressed magnetic field with their negative B_z -component still conserved inside the loop. A new magnetopause started re-forming further inside between $d = 21.50$ and $19.50 R_S$ during DOY 283. The highest spikes of the B_z -component evolved to new cut-offs for two more plasmoids that would be visible at the next Revolution (indicated by arrows in Fig. 7).

At the third return (Rev. 17, bottom panel), the interplanetary magnetic field had created new ambient conditions and made the magnetosphere cause a vast expansion. That solitary plasmoid of DOY = 282.70 had shifted by more than $10 R_S$ outward to DOY = 297.97, and faded. Other plasmoids were stretched and weakened, while the new magnetopause established at $d = 29.16 R_S$ (DOY = 299.59).

The process of restoration of the magnetopause was still continuing in the subsequent Revolution, #18. In Figure 8 we show the pulsation in a top-view on the equatorial plane. From the numbers accompanying the entry positions (diamonds) into the magnetosphere, it is seen how that boundary contracted and bounced back again at Revolutions #18 and 19.

The procedure of re-organizing would normally take place within a few hours or be completed within a day, at most. Therefore it looms unusual

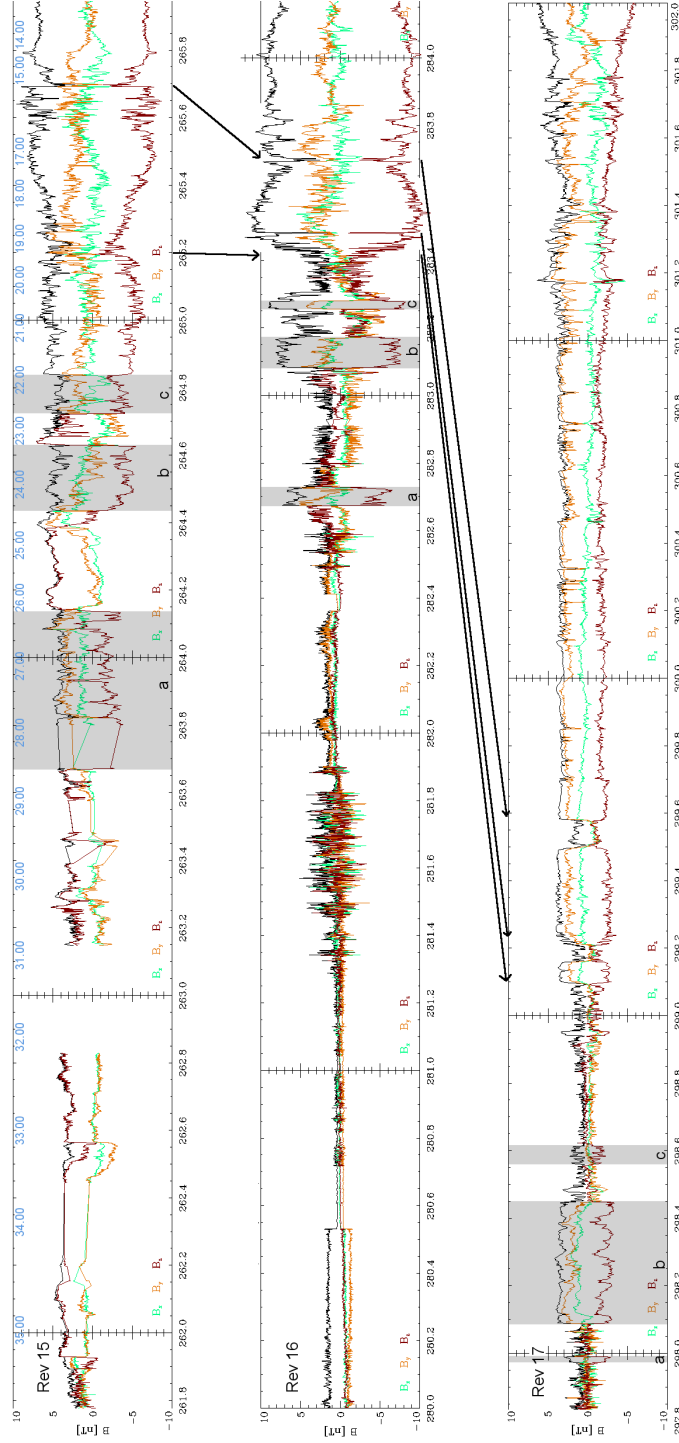


Figure 7: Magnetic field during the Revolutions 15 to 17 at the same spot of Saturnian space. The distance to Saturn is indicated at the top in blue. The modulus of the magnetic field, $|B|$, is the upper black line. The shaded areas indicate some similarities of magnetic data being stretched or compressed, respectively. The arrows show the cut-offs (reconnections) that would lead to plasmoids in the Revolution #17, bottom panel.

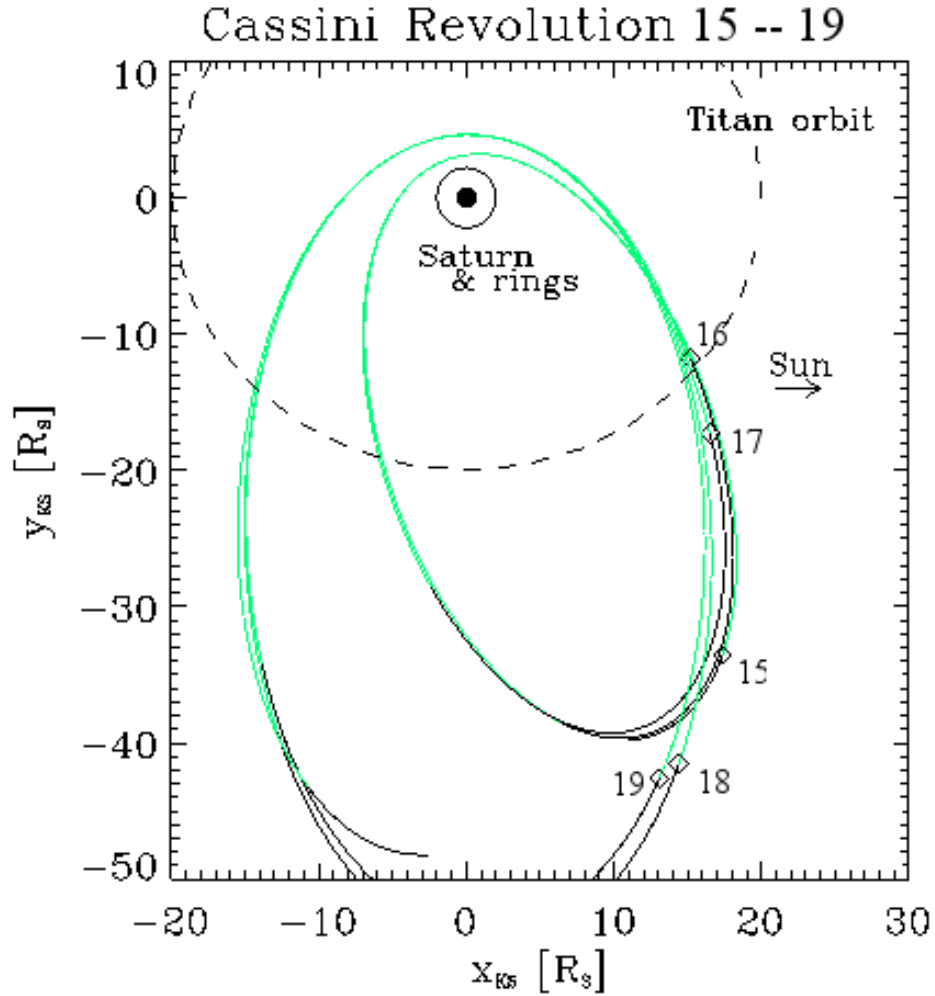


Figure 8: Trajectory for the Revolutions 015–019. The green arcs mark the space inside the magnetopause. Diamonds indicate the points of entry into Saturn’s magnetosphere.

that such magnetic relicts could remain for several days, as shown here. As [Fuselier *et al.* \(2014\)](#) point out, reconnection events are identified by two important aspects: First, their location of occurrence (planetomagnetic latitude) – this characterizes the type of reconnection in terms of the shear angle between the magnetosheath and the planet’s magnetic field at the reconnection site. And second, heated streaming electrons in the magnetosheath near the magnetopause; the electron detectors draw an abrupt change of the density and temperature when passing the magnetopause. Our explanation

of these long-lasting plasmoids (gray areas in Fig. 7) was rather interpreted as partial crossings of the magnetopause by the spacecraft.

In general, our scenario disagrees with [Bagenal & Delamere \(2011\)](#) who estimate the outflow of plasma from Saturn’s magnetodisc within one planetary rotation or less than ≈ 1 day. Therefore, we cannot exclude being erroneous and dealing with a different mechanism than suggested here. However, the similarity of the features in the shaded areas as well as the turbulence in-between appear remarkable. The patterns seem to repeat in the Revolutions #15–17, and make us suggest the same magnetic environment.

5.3. Dust-filled clouds and evacuated holes

Figure 9 reprises the initial conditions of the reconnection process in Revolution #15 in a multi-instrument view. In the uppermost panel, dust particles gather in those two blobs at DOY ≈ 264.15 –.23 and ≈ 264.67 –.75, respectively. Their impact direction is non-Keplerian, as the pointing of the CDA (yellow line) is zero. The electron density (second panel) exhibits high values matching the temperature of the solar wind; the magnetic cushion of Saturn is usually colder than these measurements. The compression of the magnetic sheath can also lead to higher thermal electrons, however, also suggesting an incipient interaction with the solar wind. These enhancements of dust and electrons coincide with a northward component of the magnetic field (third panel, red line); this component will be reconnecting and diminishing thereafter. The relicts are visible in the next orbit (middle panel of Figure 7 at DOY=282.55 and 282.76). The 10-kHz-radio signal of RPWS (green line, bottom panel) beacons to strong energetic activity. Both events are an example for a “dust-filled plasmoid” indicating a relationship of ionized nano particles with the magnetic field.

The opposite would be some kind of an “evacuated plasmoid” and is presented in Figure 10. On DOY 117/2007, *Cassini* was on its Revolution #43, a highly inclined orbit on the evening side of Saturn. It had left the magnetosphere on its outbound leg and was about $10 R_S$ above the ring plane. In the midst of the solar wind, there appeared patches of extremely low magnetic field: The first is seen at DOY = 118.06 with relicts of a magnetic turbulence centered on time stamp DOY = 118.28, and the second one starting at 118.88 till the end of the day. The CDA shows no dust impacts, except a few solitary hits. However, the pointing was excellent towards the Kepler-RAM and off, again. CAPS also suggests two hole-like features with the electron density (blue line) being depleted by three orders of magnitude. A comparison of the MAG-data revealed that the B_z -

component had a similar northward orientation, as discussed in the section above, at the respective locations during the previous orbit.

6. Discussion

The dust cloud of Revolutions #26–29 seemed to drift at a velocity of $\approx 10\text{--}14$ m/s in space. Under the assumption that Enceladus is the most significant source for permanently pouring solid material into the Saturnian space, such a cloud would need about 2.5 years to migrate from its origin to the scene of observation (Khalisi *et al.* (2015)). The frequent transits of the icy moons like Tethys, Dione, and Rhea would quickly have torn apart such a structure. The particles would be distributed along the way or stick to the surfaces of these moons. Various other effects like shock waves, gravitational drags, evaporation, and Kepler shear will also lead to a fast disruption of the cloud on the orbital time scale. Only debris larger than ≈ 1 mm in size may survive, though such large particles are not recorded.

Along with the example of a dust-filled magnetic plasmoid, we suggest the following mechanism: Nano-sized dust particles are ionized at their origin, which would be the orbit of Enceladus. This would happen due to UV-radiation or energetic jet streams. The particles become trapped inside a “magnetic cage”. Then, they will be pushed down the magnetic flow as in the model of two-cell convection by Gurnett *et al.* (2007).

Leaving behind the plasma sheet at $\approx 17 R_S$, these “cages” become isolated and turn into “plasmoids” as introduced by Goertz (1983). The plasmoids would carry the pack of tiny particles all the way through the magnetic cushion. Beyond the magnetopause they are subject to reconnection effects with the northward-oriented component of the solar magnetic field. The plasmoids burst and liberate their interior. As the swarm disrupts, the nano-particles get integrated into the ambient medium. The smallest particles vanish first, while the inert ones stay for as long as 40 days, as shown in Figure 6.

Jackman *et al.* (2014) listed some 100 plasmoids and other features in the magnetotail during 2006. Most of them lasted a few minutes, and the longest ≈ 1.5 h. The authors consider an underestimation of the plasmoid size by a factor of 4–8. Our particular dust enhancement of Figures 5 and 6 is not connected to any of their incidents. The large-scale comparison of orbits leaves us with data being almost 20 days apart. This is usually far too long for plasmoids to exist, therefore, we cannot present unambiguous footage, but a suggestion to further work.

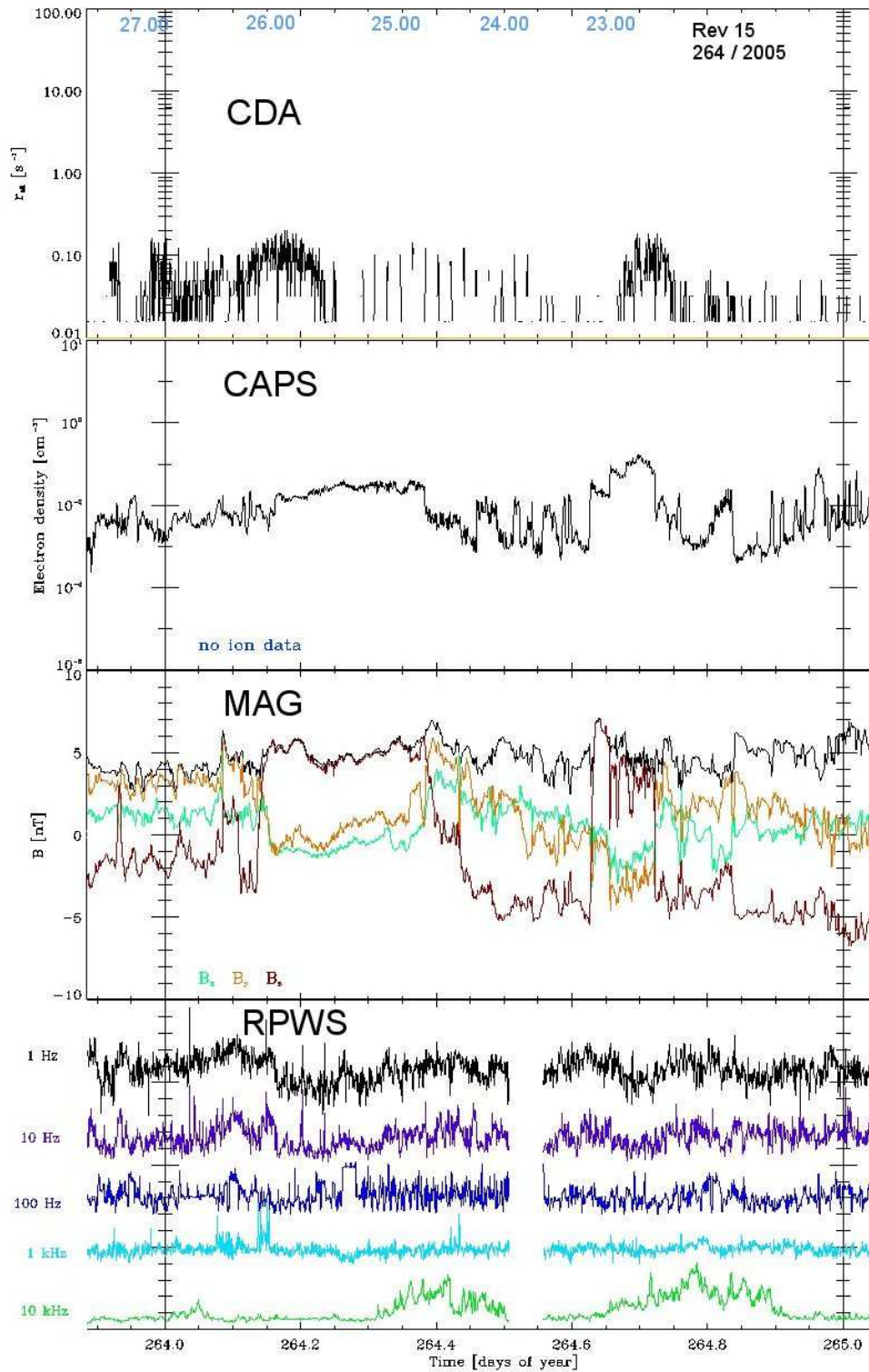


Figure 9: Multi-instrument data before entering the magnetopause on Revolution #15 at DOY = 264.72 in 2005. In the third panel, the B_z -component is colored red, while the modulus of $|\mathbf{B}|$ is the upper black line.

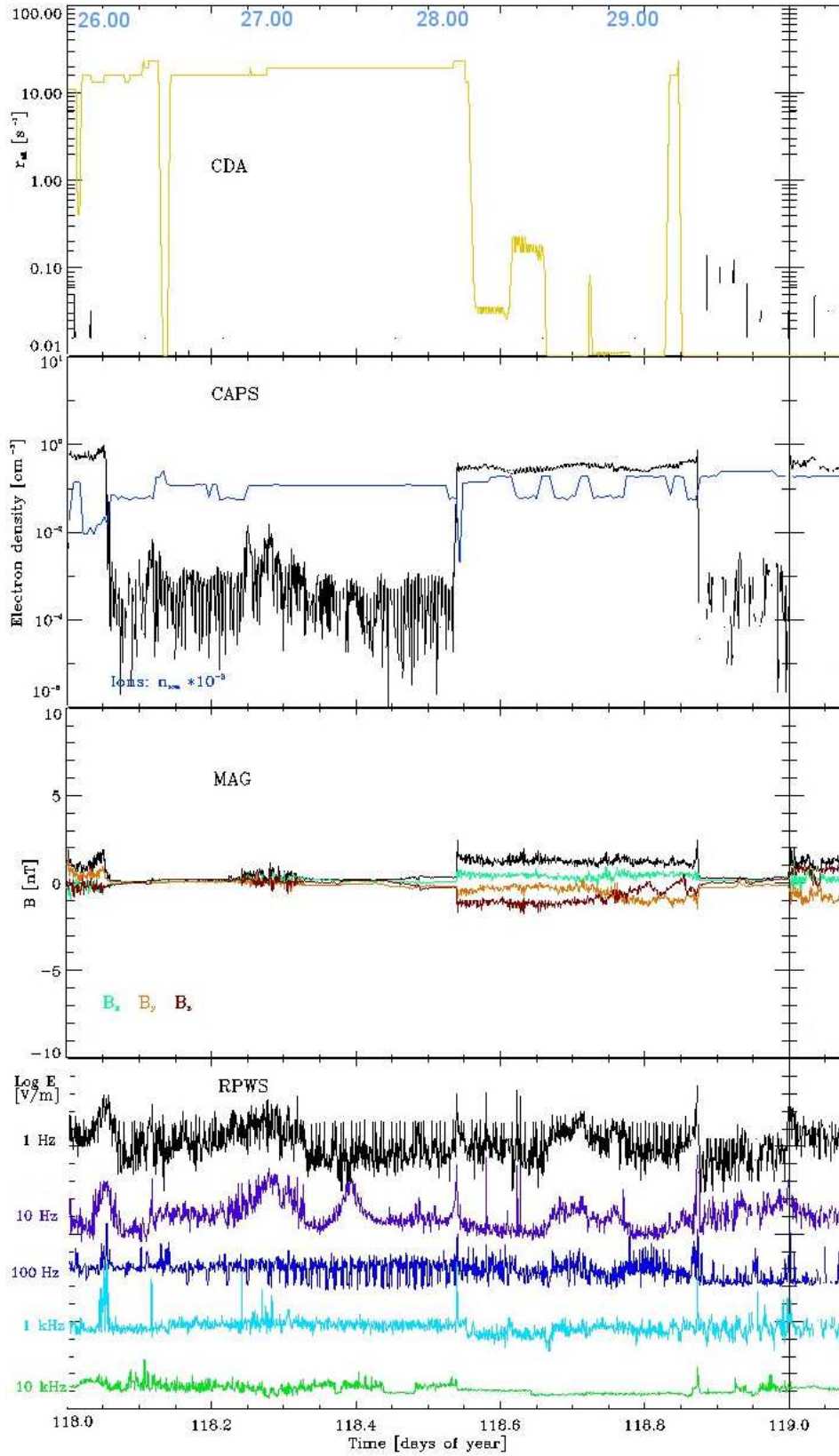


Figure 10: Dust impacts, electron density, magnetic field, and 5 low-frequency radio signals on Revolution #43 at DOY 118/2007. Distances from Saturn in R_S are indicated at the uppermost axis in blue colour.

It may be noteworthy that Krüger *et al.* (2010) also reported of surprisingly high impact rates of dust at Jupiter, when the *Galileo* spacecraft was occasionally at far-off distances from the planet. Being outside of the Jovian magnetosphere at $\approx 280 R_J$ or 0.13 Astronomical Units, an enhanced dust emission was seen and interpreted as signatures from the innermost Galilean Moon Io or its torus, respectively. That period coincided with neutral gas production from the Io torus, such that the dust particles would couple to both the gas and the magnetic field. However, the coupling mechanism was not known in detail.

An analogy can be drawn to a Coronal Mass Ejection (CME) that contains hot ions from the solar atmosphere or a prominence, in particular. As Ragot & Kahler (2003) pointed out, the electromagnetic force becomes most effective for particles smaller than 100 nm in size (their Figure 2). At the planetary distances analyzed by us, the magnetic field is much too weak for retaining the larger particles. But in the immediate vicinity of Saturn, $\leq 2 R_S$, the electrostatic interaction prevails, as the phenomenon of the dark spokes on the rings of Saturn show (Grün *et al.* (1992)). There, even micro-sized particles are caught by the strong magnetic field and forced to shift their motion.

In this paper, we suggested a heuristic mechanism that would carry a swarm of tiny particles over large distances through the magnetosphere of Saturn. However, not everybody supports the results presented here. A detailed mathematical model will be necessary to verify that view. The data of the CDA does provide the empirical basis for this. Even more such cases as in Figure 6 may be hidden in the legacy of *Cassini* and await their discovery.

Acknowledgments

We thank the Klaus Tschira Foundation, Heidelberg, for the financial support for this study from 2010 to 2013. The Max-Planck-Institute for Nuclear Physics, Heidelberg, enabled to finish the work. Thanks also to Jeffrey Kopmanis, Uni Michigan, for the help with the MAPSview data base; Harald Krüger and Norbert Krupp for discussions; and the referees for their critical comments that led to significant changes.

References

Achilleos N., Arridge C.S., Bertucci C., Jackman C.M., Dougherty M.K., Khurana K.K., Russell, C.T.: "Large-scale dynamics of Saturn's Mag-

netopause: Observations by Cassini”, *Journal of Geophysical Research* 113, A11209, 2008; doi: 10.1029/2008JA013265

André N., Blanc M., Maurice S., Schippers P., Pallier E., Gombosi T.I., Hansen K.C., Young D.T., Crary F.J., Bolton S., Sittler E.C., Smith H.T., Johnson R.E., Baragiola R.A., Coates A.J., Rymer A.M., Dougherty M.K., Achilleos N., Arridge C.S., Krimigis S.M., Mitchell D.G., Krupp N., Hamilton D.C., Dandouras I., Gurnett D.A., Kurth W.S., Louarn P., Srama R., Kempf S., Waite H.J., Esposito L.W., Clarke J.T.: ”Identification of Saturn’s Magnetospheric Regions and Associated Plasma Processes”, *Reviews of Geophysics* 46, RG4008, 2008; doi: 10.1029/2007RG000238

Arridge C.S., Russell C.T., Khurana K.K., Achilleos N., André N., Rymer A.M., Dougherty M.K., Coates A.J.: ”Mass of Saturn’s magnetodisc: Cassini observations”, *Geophysical Research Letters* 34, L09108, 2007; doi: 10.1029/2006GL028921

Arridge C.S., McAndrews H.J., Jackman C.M., Forsyth C., Walsh A.P., Sittler E.C., Gilbert L.K., Lewis G.R., Russell C.T., Coates A.J., Dougherty M.K., Collinson G.A., Wellbrock A., Young D.T.: ”Plasma electrons in Saturn’s magnetotail: Structure, distribution and energisation”, *Planetary and Space Science* 57, 2032–2047, 2009; doi: 10.1016/j.pss.2009.09.007

Bagenal F. & Delamere P.A. (2011): ”Flow of mass and energy in the magnetospheres of Jupiter and Saturn”, *Journal of Geophysical Research* 116, A05209, 2011; doi: 10.1029/2010JA016294

Banaszkiewicz M. & Krivov A.V.: ”Hyperion as a Dust Source in the Saturnian System”, *Icarus* 129, p289–303, 1997; doi: 10.1006/icar.1997.5781

Bertucci C., Duru F., Edberg N., Fraenz M., Martinecz C., Szego K., Vaisberg O.: ”The Induced Magnetospheres of Mars, Venus, and Titan”, *Space Science Reviews* 162, p113–171, 2011; doi: 10.1007/s11214-011-9845-1

Bridge H.S., Belcher J.W., Lazarus A.J., Olbert S., Sullivan J.D., Bagenal F., Gazis P.R., Hartle R.E., Ogilvie K.W., Scudder J.D., Sittler E.C., Eviatar A., Siscoe G.L., Goertz C.K., Vasyliunas V.M.: ”Plasma Observations Near Saturn: Initial Results from Voyager 1”, *Science* 212, p217–224, 1981; doi: 10.1126/science.212.4491.217

Bridge H.S., Bagenal F., Belcher J.W., Lazarus A.J., McNutt R.L., Sullivan J.D., Gazis P.R., Hartle R.E., Ogilvie K.W., Scudder J.D., Sittler

- E.C., Eviatar A., Siscoe G.L., Goertz C.K., Vasyliunas V.M.: "Plasma Observations Near Saturn: Initial Results from Voyager 2", *Science* 215, p563–570, 1982; doi: 10.1126/science.215.4532.563
- Burch J.L., Goldstein J., Lewis W.S., Young D.T., Coates A.J., Dougherty M.K., André N.: "Tethys and Dione as Sources of outward-flowing plasma in Saturn's magnetosphere", *Nature* 447, p833–835, 2007; doi: 10.1038/nature05906
- Delamere P.A., Otto A., Ma X., Bagenal F., Wilson R.J.: "Magnetic flux circulation in the rotationally driven giant magnetospheres", *Journal of Geophysical Research: Space Physics* 120, p4229–4245; doi: 10.1002/2015JA021036
- Frank L.A., Burek B.G., Ackerson K.L., Wolfe J.H., Mihalov J.D.: "Plasmas in Saturn's Magnetosphere", *Journal of Geophysical Research* 85, No. A11, p5695–5708, 1980; doi: 10.1029/JA085iA11p05695
- Fuselier S.A., Frahm R., Lewis W.S., Masters A., Mukherjee J., Petrinec S.M., Sillanpaa I.J.: "The location of magnetic reconnection at Saturn's magnetopause: A comparison with Earth", *Journal of Geophysical Research Space Physics* 119, p2563–2578, 2014; doi: 10.1002/2013JA019684
- Galopeau P.H.M. & Lecacheux A.: "Variations of Saturn's radio rotation period measured at kilometer wavelengths", *Journal of Geophysical Research* 105, No. A6, p13089–13102, 2000; doi: 10.1029/1999JA005089
- Goertz C.K.: "Detached Plasma in Saturn's Front Side Magnetosphere", *Geophysical Research Letters* 10, p455–458, 1983; doi: 10.1029/GL010i006p00455
- Goldreich P. & Farmer A.J.: "Spontaneous axisymmetry breaking of the external magnetic field at Saturn", *Journal of Geophysical Research* 112, A05225, 2007; doi: 10.1029/2006JA012163
- Grün E., Goertz C.K., Morfill G.E., Havnes O.: "Statistics of Saturn's Spokes", *Icarus* 99, p191–201, 1992; doi: 10.1016/0019-1035(92)90182-7
- Grün E., Dikarev V., Frisch P.C., Graps A., Kempf S., Krüger H., Landgraf M., Moragas-Klostermeyer G., Srama R.: "Dust in Interplanetary Space and in the Local Galactic Environment", *ASP Conference Series* 309, 2004, p245–264; in: *Astrophysics of Dust*, Edited by Witt A.N., Clayton G.C., and Draine B.T., ISBN 978-1-58381-244-0

- Gurnett D.A., Persoon A.M., Kurth W.S., Groene J.B., Averkamp T.F., Dougherty M.K., Southwood D.J.: "The Variable Rotation Period of the Inner Region of Saturn's Plasma Disk", *Science* 316, 2007, p442; doi: 10.1126/science.1138562
- Hartle R.E., Sittler E.C., Ogilvie K.W., Scudder J.D., Lazarus A.J., Atreya S.K.: "Titan's Ion Exosphere Observed From Voyager 1", *Journal of Geophysical Research* 87, A3, p1383–1394, 1982; doi: 10.1029/JA087iA03p01383
- Hill T.W.: "Interchange stability of a rapidly rotating magnetosphere", *Planetary and Space Science* 24, p1151–1154, 1976; doi: 10.1016/0032-0633(76)90152-5
- Hill T.W., Thomsen M.F., Henderson M.G., Tokar R.L., Coates A.J., McAndrews H.J., Lewis G.R., Mitchell D.G., Jackman C.M., Russell C.T., Dougherty M.K., Cray F.J., Young D.T.: "Plasmoids in Saturn's magnetotail", *Journal of Geophysical Research* 113, A01214, 2008; doi: 10.1029/2007JA012626
- Jackman C.M., Slavin J.A., Kivelson M.G., Southwood D.J., Achilleos N., Thomsen M.F., DiBraccio G.A., Eastwood J.P., Freeman M.P., Dougherty M.K., Vogt M.F.: "Saturn's dynamic magnetotail: A comprehensive magnetic field and plasma survey of plasmoids", *Journal of Geophysical Research* 119, 5465–5494, 2014; doi: 10.1002/2013JA019388
- Kennedy G.M., Wyatt M.C., Su K.Y.L., Stansberry J.A.: "Searching for Saturn's dust swarm: limits on the size distribution of irregular satellites from km to micron sizes", *Monthly Notices RAS* 417, p2281–2287, 2011; doi: 10.1111/j.1365-2966.2011.19409.x
- Khalisi E., Srama R., Grün E.: "Counter data of the Cosmic Dust Analyzer aboard the Cassini spacecraft and possible 'dust clouds' at Saturn", *Advances in Space Research* 55, p303–310, 2015; doi: 10.1016/j.asr.2014.09.002
- Krivov A.V. & Banaszekiewicz M.: "Unusual origin, evolution and fate of icy ejecta from Hyperion", *Planetary and Space Science* 49, p1265–1279, 2001; doi: 10.1016/S0032-0633(01)00069-1
- Krüger H., Bindschadler D., Dermott S.F., Graps A.L., Grün E., Gustafson B.A., Hamilton D.P., Hanner M.S., Horányi M., Kissel J., Linkert D.,

Linkert G., Mann I., McDonnell J.A.M., Moissl R., Morfill G.E., Polanskey C., Roy M., Schwehm G., Srama, R.: "Galileo dust data from the jovian system: 2000 to 2003", *Planetary and Space Science* 58, p965-993, 2010; doi: 10.1016/j.pss.2010.03.003

Porco C.C., Helfenstein P., Thomas P.C., Ingersoll A.P., Wisdom J., West R., Neukum G., Denk T., Wagner R., Roatsch T., Kieffer S., Turtle E., McEwen A., Johnson T.V., Rathbun J., Veverka J., Wilson D., Perry J., Spitale J., Brahic A., Burns J.A., Del Genio A.D., Dones L., Murray C.D., Squyres S.: "Cassini Observes the Active South Pole of Enceladus", *Science* 311, p1393-1401, 2006; doi: 10.1126/science.1123013

Ragot B.R. & Kahler S.W.: "Interactions of Dust Grains with Coronal Mass Ejections and Solar Cycle Variations of the F-Coronal Brightness", *The Astrophysical Journal* 594, p1049-1059, 2003; doi: 10.1086/377076

Sittler E.C. jr., Ogilvie K.W., Scudder J.D.: "Survey of Low-Energy Plasma Electrons in Saturn's Magnetosphere: Voyagers 1 and 2", *Journal of Geophysical Research* 88, p8847-8870, 1983; doi: 10.1029/JA088iA11p08847

Szego K., Bebesi Z., Erdos G., Foldy L., Crary F., McComas D.J., Young D.T., Bolton S., Coates A.J., Rymer A.M., Hartle R.E., Sittler E.C., Reisenfeld D., Bethelier J.J., Johnson R.E., Smith H.T., Hill T.W., Vilppola J., Steinberg J., Andre N.: "The global plasma environment of Titan as observed by Cassini Plasma Spectrometer during the first two close encounters with Titan", *Geophysical Research Letters* 32, L20S05, 2005, doi: 10.1029/2005GL022646